Effect of Implanting a Soft Tissue Autograft in a Central-Third Patellar Tendon Defect: Biomechanical and Histological Comparisons

Kirsten R. C. Kinneberg[1]
University of Cincinnati,
School of Energy, Environmental,
Biological and Medical Engineering,
Biomedical Engineering Program,
2901 Woodside Drive,
601 Engineering Research Center,
Cincinnati, OH 45220
e-mail: Kirsten.kinneberg@gmail.com

Marc T. Galloway
Cincinnati SportsMedicine & Orthopaedic Center,
7423 Mason-Montgomery Rd.,
Mason, OH 45040-8082
e-mail: mgalloway@csmoc.com

David L. Butler
e-mail: david.butler@uc.edu

Jason T. Shearn
e-mail: jason.shearn@uc.edu

University of Cincinnati,
School of Energy, Environmental,
Biological and Medical Engineering,
Biomedical Engineering Program,
2901 Woodside Drive,
601 Engineering Research Center, ML0048,
Cincinnati, OH 45220

Previous studies by our laboratory have demonstrated that implanting a stiffer tissue engineered construct at surgery is positively correlated with repair tissue stiffness at 12 weeks. The objective of this study was to test this correlation by implanting a construct that matches normal tissue biomechanical properties. To do this, we utilized a soft tissue patellar tendon autograft to repair a central-third patellar tendon defect. Patellar tendon autograft repairs were contrasted against an unfilled defect repaired by natural healing (NH). We hypothesized that after 12 weeks, patellar tendon autograft repairs would have biomechanical properties superior to NH. Bilateral defects were established in the central-third patellar tendon of skeletally mature (one year old), female New Zealand White rabbits ($n=10$). In one limb, the excised tissue, the patellar tendon autograft, was sutured into the defect site. In the contralateral limb, the defect was left empty (natural healing). After 12 weeks of recovery, the animals were euthanized and their limbs were dedicated to biomechanical ($n=7$) or histological ($n=3$) evaluations. Only stiffness was improved by treatment with patellar tendon autograft relative to natural healing ($p=0.009$). Additionally, neither the patellar tendon autograft nor natural healing repairs regenerated a normal zonal insertion site between the tendon and bone. Immunohistochemical staining for collagen type II demonstrated that fibrocartilage-like tissue was regenerated at the tendon-bone interface for both repairs. However, the tissue was disorganized. Insufficient tissue integration at the tendon-to-bone junction led to repair tissue failure at the insertion site during testing. It is important to re-establish the tendon-to-bone insertion site because it provides joint stability and enables force transmission from muscle to tendon and subsequent loading of the tendon. Without loading, tendon mechanical properties deteriorate. Future studies by our laboratory will investigate potential strategies to improve patellar tendon autograft integration into bone using this model. [DOI: 10.1115/1.4004948]

Keywords: insertion site, autograft, central-third patellar tendon, natural healing

Introduction

Tendon injury represents a significant clinical challenge in orthopaedic and sports medicine. While treatments such as direct repair and autograft or allograft replacement are viable options, the occurrence of re-rupture and post-operative complications is often high [1–6]. As injury rates rise and the number of primary reconstructions increases, the need for revision surgery is likely to increase as well [7]. These issues present a clear need to improve traditional tendon repair strategies.

Currently, multiple strategies are being studied to enhance tendon repair. One strategy is treatment with growth factors [8–12]. Despite the positive result of increasing repair tissue structural properties relative to untreated and/or sham controls [8,10–12], growth factor treatments appear to promote large amounts of poor quality scar tissue rather than regenerated tendon [9,10]. Another approach is to augment repairs by reinforcing sutures with various biologic scaffolds (i.e. CuffPatch [Arthrotek, Warsaw, IN], Restore [Depuy, Warsaw, IN], etc) [13–15]. Augmentation grafts increase suture fixation strength compared to un-augmented repairs and the biochemical composition of the grafts is similar to that of tendon [14]. However, the discrepancy between elastic moduli of grafts and native tendon limits their mechanical role in augmenting tendon repair [13]. To offer both a biological and mechanical component to tendon repair strategies, researchers are developing tissue engineered constructs (TECs).

Our laboratory has focused on TECs composed of collagen-based scaffolds and mesenchymal stem cells (MSCs) to repair tendon defects [16–21]. When implanted into a central-third patellar tendon (PT) defect in the rabbit, mechanically stimulated MSC-collagen sponge TECs produced 12-week repairs that matched the tangent stiffness of normal patellar tendon up to 32% of failure force or 50% greater than the loads and displacements required for normal activities of daily living [18]. Additionally, paired in vitro-in vivo studies found that in vitro TEC stiffness was significantly and positively correlated with repair tissue stiffness 12 weeks after surgery [18,19]. Our results suggest that repairing a central-third PT defect with a stiffer implant will promote a better repair outcome.

To examine if further increases in implant stiffness would continue to enhance tendon repair, we filled the central-third PT defect with a TEC that matches normal tissue biomechanics, the soft tissue patellar tendon autograft (PTA). We hypothesized that after 12 weeks of recovery, the PTA would produce repair tissue with biomechanics superior to natural healing (NH). Additionally, when compared to our previous studies [17,18], we hypothesized that PTA repair tissue biomechanical properties would be superior to repairs using TECs but inferior to the normal central-third PT.

[1]Corresponding author.

Contributed by the Bioengineering Division of ASME for publication in the JOURNAL OF BIOMECHANICAL ENGINEERING. Manuscript received June 21, 2011; final manuscript received August 23, 2011; published online October 4, 2011. Editor: Michael Sacks.

Materials and Methods

Experimental Design. All procedures were approved by the University of Cincinnati Institutional Animal Care and Use Committee. Full-length, full-thickness, central-third PT defects with patellar and tibial bony defects were created in both limbs of ten one-year-old, skeletally mature, female New Zealand White rabbits. Defects were either repaired by suturing the excised PT to the remaining medial/lateral struts (PT autograft, PTA) or left unfilled (natural healing, NH). After 12 weeks of recovery, repair tissues were harvested for biomechanical ($n=7$) and histological evaluations ($n=3$). Tendons for biomechanical evaluation were dissected down to the central-third repair tissue and failed in uniaxial tension at a constant strain rate (20%/sec). Tendons for histological evaluation were processed and stained with hematoxylin and eosin (H&E) along with antibodies for collagen types II (bone ends only) and III (mid-substance only). Patella and tibial bone ends were stained with antibodies for collagen type II because it is the primary structural protein of fibrocartilage found at the tendon-to-bone insertion site. Mid-substance sections were stained with antibodies for collagen type III because it is an important structural protein during healing.

Surgical Procedure and Limb Harvest. At surgery, each rabbit was anesthetized with an anesthesia cocktail of ketamine/acepromazine (40 mg/kg and 5 mg/kg, respectively) and isoflurane gas (as needed). Under aseptic conditions, each patellar tendon was exposed through an anteromedial incision. A 3 mm wide, full-length, full-thickness, central-third defect was created in each PT, producing a soft tissue, patellar tendon autograft (PTA). Bone defects were created at the proximal and distal insertion sites using a pneumatic sagittal saw (MicroAire Surgical Instruments, Charlottesville, VA). In the right limb, the excised PTA was sutured back into the defect at four sites (Prolene 5-0, Ethicon, Somerville, NJ): two each near the patella and tibia. In the contralateral limb, the defect remained unfilled (natural healing, NH). Each incision was closed with a continuous subcutaneous suture followed by simple interrupted sutures in the skin. After recovering from anesthesia, each animal was returned to its cage and allowed unrestricted cage activity. Twelve weeks post-surgery, each rabbit was anesthetized as described above and then euthanized by intracardiac administration of Euthasol® (1.0 cc/4.54 kg; Virbac Animal Health, Inc., Fort Worth, TX) followed by bilateral pneumothorax. Hind limbs were disarticulated at the hip and removed using a scalpel. For biomechanical evaluation, whole limbs were stored at −20 °C for approximately two weeks until testing. For histological evaluation, patella-PT-tibia samples were placed in 10% neutral buffered formalin and stored at room temperature (25 °C) until further processing.

Biomechanical Evaluation. One day prior to testing, limbs were removed from the freezer and allowed to thaw overnight. On the day of testing, all extraneous tissues (including the infrapatellar fat pad) were removed leaving only the patella, patellar tendon (PT) and tibia. The length and width of the whole PT were measured at the medial/central/lateral and proximal/central/distal portions of the tendon, respectively, using dial calipers (Mitutoyo, Aurora, IL). Tendon length was measured on the posterior surface from tibial insertion to patellar insertion. Due to the ellipsoidal shape of the PT, whole PT width and thickness are reported by region (proximal/central/distal). Thickness of the whole PT was measured at the proximal/central/distal portions of the tendon using a light force (<0.15 N) digital micrometer (accurate to 0.01 mm; IDC type Mitutoyo Digimatic Indicator, MTI Corp., Aurora, IL). The native tendon struts were removed to isolate the central-third repair tissue. The tibia/fibula complex was cut roughly 2.5 cm distal to the tibial tuberosity to create a bone block. The length, width and thickness of the patella-central-third repair-tibia samples were then measured as described for the whole PT. Patellar and tibial bone blocks were fixed into custom designed grips using polymethylmethacrylate cement (Dentsply International, York, PA) [18,22]. The testing grips for each sample were secured into a Plexiglas tank mounted on a materials testing system (Model 8501, Instron, Inc., Canton, MA). The tank contained phosphate buffered saline (PBS; *p*H 7.4) heated to 37 °C. Repair tissues were preloaded to 14.8 ± 8.8 N (mean ± SD) and then preconditioned for 50 cycles to 3% strain at 1 Hz using a sinusoidal strain pattern. Tissues were then failed in uniaxial tension at a constant strain rate of 20%/sec while force and displacement were continuously recorded [18,21–23].

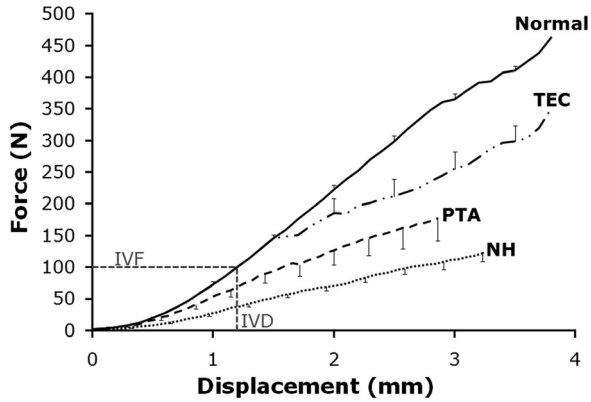

Fig. 1 Force-displacement curves (mean ± SEM). PTA ($n=6$) and NH ($n=6$) repairs both exceeded the peak in vivo force required for activities of daily living (100 N; in vivo force and displacement, IVF and IVD, respectively) [29,30]. However, PTA and NH repairs do not match the normal central-third PT (Normal; $n=8$ [17,18]) or TEC ($n=7$ [18]) repair curves. Portions of this figure re-printed with permission from Juncosa-Melvin, et al. (2006) [18].

Histological Evaluation. Tissue processing has been described previously [24] but a brief protocol is outlined below. Fixed patella-PT-tibia samples were sectioned in the transverse plane to isolate a) the patella and proximal PT, b) the tendon

Table 1 Repair Tissue Dimensions [mean (SEM)] for Whole and Central-Third PT

	Whole PT									
		Width (mm)			Thickness (mm)			Central-Third PT		
	Length (mm)	Proximal	Central	Distal	Proximal	Central	Distal	Length (mm)	Width (mm)	Thickness (mm)
NH	18.7	9.6	10.4	10.4	2.0	2.0	2.2	19.2	2.5	1.5
($n=6$)	(0.5)	(0.2)	(0.7)	(0.7)	(0.2)	(0.2)	(0.2)	(0.4)	(0.2)	(0.1)
PTA	20.7	9.9	11.5	11.8	2.7*	2.6*	3.0*	21.4	3.0*	2.2*
($n=6$)	(0.9)	(0.7)	(0.5)	(0.8)	(0.2)	(0.2)	(0.2)	(1.0)	(0.1)	(0.1)

*Significantly greater than NH repair values ($p<0.05$)

mid-substance, and c) the tibia and distal PT. Patellar and tibial bone ends were decalcified in 10% formic acid. Each tissue section was then dehydrated through a gradient of alcohols and xylene before being embedded in a paraffin block. The bony ends (patella and proximal PT, tibia and distal PT) were processed by cutting eight serial sections (4 μm thick) in the sagittal plane at 1 mm intervals through the sample. These tissues were used to examine tendon integration into bone and insertion site formation. The mid-substance samples were processed by cutting eight serial sections in the coronal plane at 250 μm intervals. These tissues were used to examine PTA and NH integration into the tendon native struts. One section from each depth was stained with H&E. Select serial sections were then subjected to immunohistochemical (IHC) staining for collagen type II (Calbiochem, San Diego, CA) and collagen type III (Sigma-Aldrich, St. Louis, MO). Repair tissue organization, cellularity, neovascularization, repair tissue integration into the native tendon struts, and tendon-bone insertion site formation were evaluated by one of the authors (KRCK).

Statistical Analysis. One animal sustained a unilateral rupture of its left limb (natural healing treatment group). In a separate animal, the biomechanical properties of the right limb (PTA treatment group) were statistical outliers. These two limbs were excluded from statistical analysis leaving a sample size of $n=6$ per treatment group. Data were normal and homoscedastic. Differences in dimensional ($n=6$) and biomechanical ($n=6$) data were assessed using a one-way ANOVA with repair treatment as a fixed factor. The significance level was set at $p<0.05$.

Results

Repair Tissue Dimensions. After 12 weeks of healing, both whole PT and central-third repair tissue dimensions were significantly affected by repair treatment (NH versus PTA; Table 1). Compared to NH, treatment with the PTA significantly increased: 1) whole PT thickness by 35%, 30% and 36% in the proximal, central, and distal regions, respectively ($p \leq 0.044$); 2) whole PT cross-sectional area by 46% in the distal region ($p=0.025$); and 3) central-third repair tissue width, thickness, and cross-sectional area by 20%, 47%, and 78%, respectively ($p \leq 0.011$).

Repair Tissue Biomechanical Properties and Failure Mechanisms. Treatment with PTA significantly enhanced repair tissue stiffness, as compared to NH, at 12 weeks post-surgery ($p=0.006$; Fig. 1, Table 2). However, maximum force, maximum stress and modulus were not affected by repair treatment. Of the six PTA repairs tested, five failed at the patellar insertion site (83.3%) and one failed in the mid-substance (16.7%). By contrast, of the six NH repairs tested, three failed at the patellar insertion site (50%) and three failed in the mid-substance (50%). All samples failed at the insertion site with no detectable bone avulsion for any of the samples.

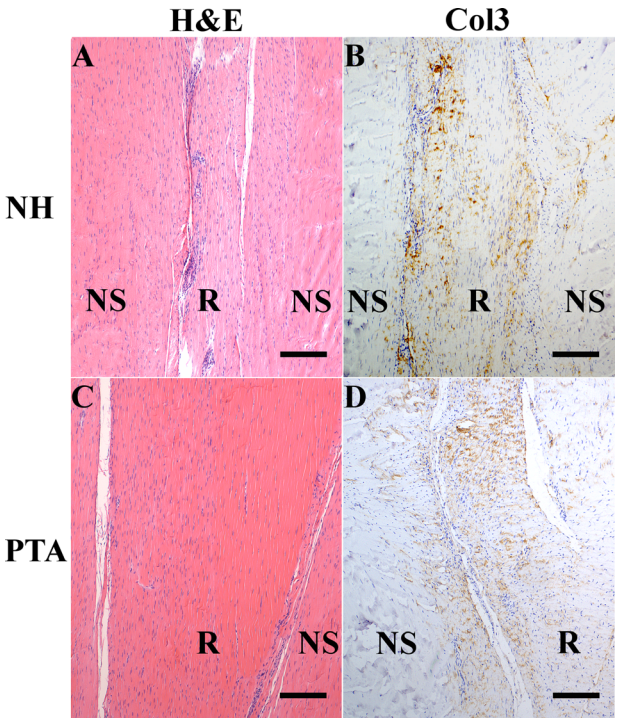

Fig. 2 H&E staining and IHC staining for collagen type III (Col3) of the tendon mid-substance for both NH and PTA after 12 weeks of healing. Col3 (brown) is primarily localized to the central-third repairs tissue (R) for natural healing (NH) samples and localized to the graft-native strut (NS) interface for PTA samples. Neo-vascularization is visible in the native struts (NS) and central-third repair (R) regions for both tissues (the central-third repair is labeled as R for both NH and PTA samples). Scale bar = 200 μm.

Tendon Repair Mid-Substance Histology. PTA and NH repair mid-substance tissues showed several similarities (Fig. 2). First, PTA and NH central-third repair tissues contained regions of neo-vascularization and hypercellularity, as did the native struts. Second, PTA and NH samples contained regions with aligned tissue showing some evidence of a crimp pattern along with both rounded and elongated cell nuclei. Lastly, a band of hypercellular tissue was present at both the graft and natural healing-native strut interfaces for PTA and NH samples, respectively.

Histological examination also revealed differences between PTA and NH samples. While both central-third repairs appeared hypercellular relative to normal, NH repairs appeared more hypercellular than PTA repairs (Fig. 2). Additionally, collagen type III staining was primarily localized to the graft-native tissue interface

Table 2 Biomechanical Properties (Mean ± SEM) of Natural Healing, Patellar Tendon Autograft, Tissue Engineered Construct and Normal Central-Third PT

	NH ($n=7$)	PTA ($n=7$)	TEC[a] ($n=7$)	Normal[b] ($n=8$)
Max Force (N)	121.8 ± 13.0[d,e]	154.2 ± 20.1[d,e]	339.3 ± 10.9[e]	470.7 ± 23.8
Stiffness (N/mm)	52.0 ± 4.3[c,d,e]	74.2 ± 4.6[d,e]	141.6 ± 3.2	159.8 ± 11.1
Max Stress (MPa)	34.9 ± 4.9[d,e]	23.7 ± 3.3[d,e]	72.0 ± 1.8[e]	100.7 ± 5.6
Modulus (MPa)	286.0 ± 36.8[d,e]	243.4 ± 17.1[d,e]	441.1 ± 3.1[e]	861.4 ± 98.5

[a]TEC repair tissue biomechanical properties were previously obtained [18]
[b]Normal central-third PT biomechanical properties were previously obtained [17,18]
[c]Significantly less than PTA repair ($p<0.05$)
[d]Significantly less than TEC repair ($p \leq 0.05$)
[e]Significantly less than normal central-third ($p \leq 0.05$)

in PTA repair samples (Fig. 2(*d*)) but was found throughout the repair tissue in NH samples (Fig. 2(*b*)).

Patellar and Tibial Insertion Site Histology. Although PTA and NH repairs showed similar results at the patellar and tibial insertions, neither repair matched the zonal insertion appearance of the native struts. The PTA and NH repair tissues were morphologically different than the native struts in the tendon adjacent to the enthesis, the fibrocartilage and the underlying bone. In the native strut, the tendon adjacent to the enthesis contained parallel rows of tenocytes that gradually transitioned into parallel rows of tendon fibers separated by rows of fibrochondrocytes (Fig. 3, bottom row). The tendon fibers in the PTA and NH repairs adjacent to the enthesis were generally disorganized or oriented parallel to the bone surface (Fig. 3, middle row and top row, respectively). IHC staining revealed the presence of type II collagen in the fibrocartilage region of PTA repairs, NH and native struts at both the patellar and tibia entheses. However, the fibrocartilage region of the native struts contained rows of fibrochondrocytes separated by collagen fibers anchoring into the underlying bone and was composed of visible layers of fibrocartilage (FC) and mineralized fibrocartilage (MFC) separated by a basophilic tidemark (Fig. 3, bottom row). While the fibrocartilage region of PTA repairs was more organized than NH, neither group regenerated distinct FC/MFC zones or a tidemark. Additionally, the fibrocartilage regions of the PTA and NH samples contained disorganized fibrochondrocytes with no evidence of tendon fibers actually passing through the enthesis and anchoring into bone (Fig. 3, middle row and top row, respectively). In the native strut, compact bone was adjoined to the fibrocartilage region. In PTA repairs and NH, discontinuities were found in the compact bone. The underlying bone for both PTA repairs and NH contained bone marrow cavities and exhibited a more trabecular appearance, thus signs of remodeling, which were not evident in the native strut.

Discussion

Our first hypothesis, that after 12 weeks of recovery, the PTA would produce repair tissue with biomechanical properties superior to NH, was only correct for stiffness. The finding that maximum force, maximum stress, and modulus were not statistically different for NH and PTA repairs is likely due to poor tendon-to-bone integration at the patellar and tibial entheses. Relative to NH, treatment with the PTA increased insertion site failure frequency from ~50% to ~83%. Therefore, it is possible that the PTA repair tissue mid-substance was biomechanically superior to that for NH but, because normal insertion sites were not regenerated, the PTA repairs failed at their weakest link before the mid-substance tissue could be loaded to failure to determine its biomechanical properties.

There are several possible reasons for why the NH and PTA repairs failed to regenerate normal, zonal entheses: 1) The rabbits were only given 12 weeks to recover. Both Rodeo, et al. [25] and Wong, et al. [26] have demonstrated in multiple injury models that animals may need a longer recovery period (24–26 weeks post-surgery) to allow soft tissue-to-bone healing to mature [25,26].

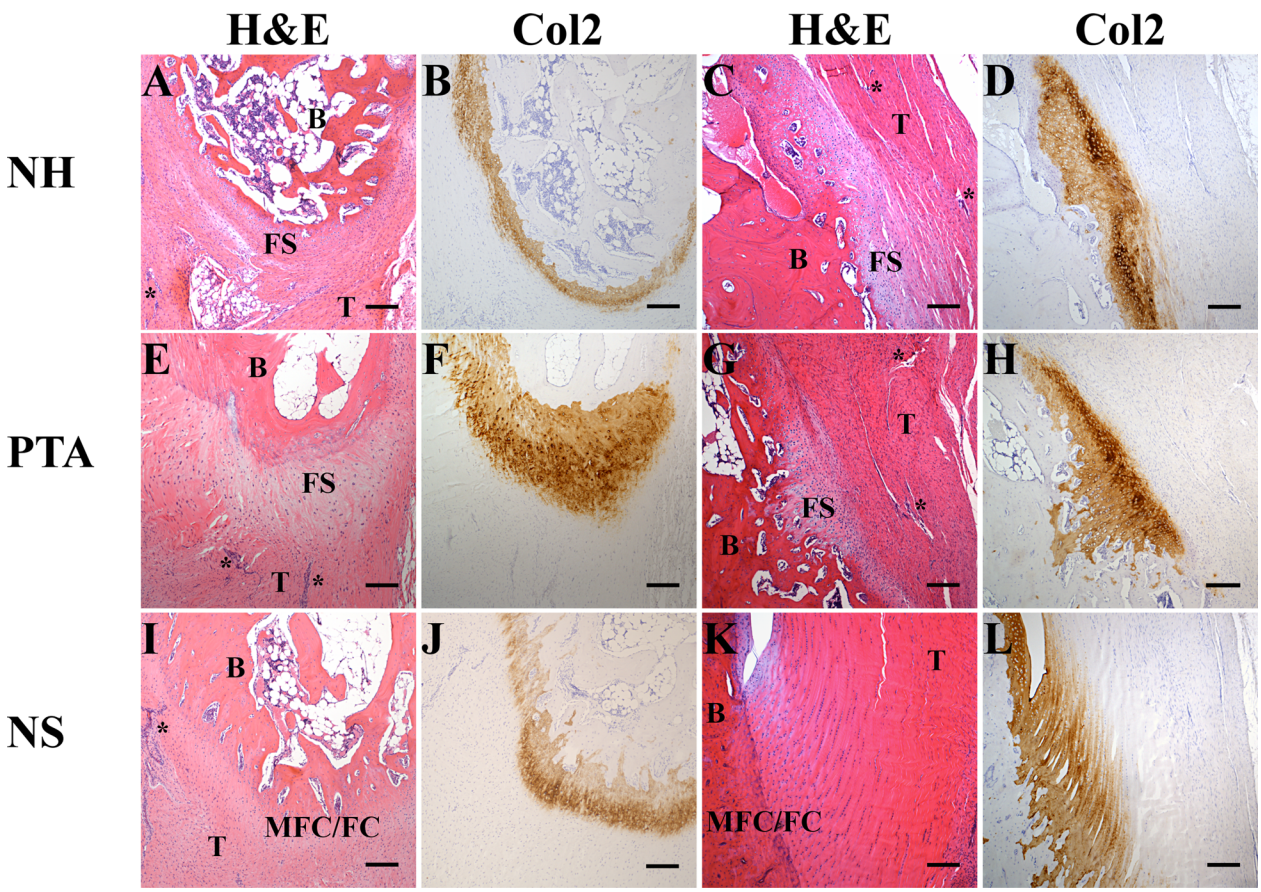

Fig. 3 Histological images of patellar and tibial tendon-to-bone insertion sites. Insertion site images are shown with H&E staining and immunohistochemical staining for type II collagen (Col2). After 12 weeks of healing, proper insertion sites were not regenerated by PTA or NH. The insertion sites in the native struts (NS) appear unaffected by the surgical procedure. H&E images are labeled to reflect: B, bone; T, tendon; FS, fibrous scar; MFC/FC, mineralized fibrocartilage/fibrocartilage zones of the insertion site, respectively (note: these zones are not as distinct in the patella as they are in the tibia); areas resembling neo-vascularization are marked with an asterisk. Scale bar = 200 μm.

Our future studies will examine the effect of a longer recovery time on both repair tissue biomechanical properties and insertion site formation. 2) The tendon-to-bone insertion site may not be exposed to the optimal mechanical environment for proper healing. While early protected passive mobilization can enhance the strength of repaired tendons [27], early immobilization may provide a protective environment for tendon integration into bone that drives the healing response toward regeneration rather than scar tissue formation [10,25,28]. 3) The biological cues necessary to promote bone ingrowth and tendon incorporation may have been absent or present at insufficient levels [10]. These biological cues include, but are not limited to, bone morphogenic proteins [8,10], collagen types I and II [28], and alkaline phosphatase activity [28]. Future studies will examine how incorporating chemically and/or mechanically preconditioned biological augmentations at the insertion sites might enhance tendon integration into bone.

Our second hypothesis was that the PTA repair tissue biomechanical properties would be superior to our previous repairs using TECs but inferior to the normal central-third patellar tendon. This hypothesis was rejected. While we expected the average force-displacement curve for NH to be significantly lower than our best TEC repair [18], we were surprised to find that the average PTA force-displacement curve was also significantly less than our best TEC repair [18] (Fig. 1; Table 2). PTA and NH repairs both exceeded the peak in vivo force required for activities of daily living (100 N) [29,30], which is one of our criteria for a successful repair. However, neither PTA repair nor NH matched the tangent stiffness of the normal PT in the functional range of loading (Fig. 1, lower left corner), which is another one of our criteria for success. Overall, the repair tissue biomechanics of our mechanically preconditioned MSC-collagen sponge TECs were approximately twice the biomechanical properties of both PTA repairs and NH (Table 2).

Three factors that may explain why the TEC produced superior repair tissue biomechanics relative to the PTA are the cell population, the porosity, and the compliance of the respective implants. The TEC contained bone marrow-derived MSCs that had been mechanically preconditioned in culture. When compared to static culture, mechanical stimulation of MSC-collagen sponge TECs increased mRNA expression levels of collagen types I and III [20], which each play an important role in tendon healing. In contrast, the resident cell population of the PTA was likely composed primarily of mature tenocytes with lower metabolic activity [31]. While it is possible that the tenocytes reverted back to their highly metabolic state as tenoblasts, it is also possible that the autograft tissue underwent a phase of necrosis and hypocellularity, similar to what is seen during ligamentization of grafts for ACL replacement [32,33]. Additionally, the porous microstructure of the MSC-collagen sponge TEC may offer the advantage of rapid cellular infiltration and easier integration with the native struts. It is also possible that without early integration at the autograft-native strut interfaces, the PTA was stress shielded by the native struts and thereby not exposed to sufficient forces to promote significant tissue remodeling [34–36]. Additionally, because the TEC is more compliant than the PTA, it may take less force to stretch the implant and overcome the detrimental effects immobilization can have on tendon tissues [37,38].

The biomechanical and histological properties of PTA repair were consistent with those of other investigators while the biomechanical properties of NH were not. Biomechanically, the structural properties of PTA repair reached 33–46% of normal at 12 weeks post-surgery (Table 2). While a direct comparison to other PTA repairs was not possible, it has been reported for ACL reconstruction in animal models that even at one year post-surgery (or longer), the structural properties of the implanted graft do not achieve more than 50–60% of the native tissue [33,39–41]. Histologically, the following trends were consistent across several models of tendon-to-bone healing, including a partial patellectomy performed in the goat [26], a long digital extensor tendon transplantation into a bone tunnel in the tibial metaphysis in a dog [25], and a infraspinatus tendon reconstruction in the sheep rotator cuff [8]. At 12 weeks: 1) tendon fibers showed alignment along the axis of applied load, 2) some tendon fibers were continuous with bone but a zonal insertion was not regenerated, and 3) fibrous scar tissue was evident at the bone-tendon junction [8,25,26]. It was not until 24–26 weeks post-surgery that: 1) distinct fibrocartilage and mineralized fibrocartilage zones and a tidemark became evident, and 2) tendon fibers were consistently anchored into the underlying bone [25,26]. While both PTA repair and NH were biomechanically inferior to normal, the structural properties reported here for NH were up to 2.9x greater than values reported by both Miyashita et al. [42] and Awad et al. [17] for regenerated central-third patellar tendon in the rabbit. One key differentiating factor, which may explain the discrepancy in structural properties, is that both Miyashita et al. [42] and Awad et al. [17] secured suture markers at the periphery of the defect site while we did not. The sutures may have prolonged the inflammatory response and thus delayed the remodeling phase of healing that is responsible for increasing biomechanical properties.

Our study is not without limitations. 1) Our model does not replicate graft replacement or surgical reconstruction of a tendon or ligament tear. Our model does, however, provide a reproducible and accessible system to test tissue engineering strategies to promote tendon healing and integration into bone. 2) The current sample size did not allow us to make a definitive statistical conclusion about the maximum force sustained by PTA repairs and NH samples at 12 weeks. However, both repair methodologies are statistically inferior to TEC-based repairs and vast improvements are needed to produce a viable repair using the PTA.

This study demonstrates that a soft tissue PTA generates repair tissue that is generally equivalent to NH but inferior to both TEC repair and normal tendon. Biomechanical results show PTA repairs possess inadequate tissue stiffness in the functional range of loading and fail near the insertion into bone. Histological results demonstrate incomplete integration of the PTA soft tissue into bone and affirm that the tendon-to-bone insertion is the weak link of the repair. Using the model presented here, our laboratory can now investigate potential strategies to improve the integration of tendon into bone. Future studies will examine novel ways to improve tendon-to-bone insertional repair, including MSC-gel TECs that have previously produced ectopic bones spicules in vivo [17].

Acknowledgment

The authors thank Cynthia Gooch, Nathaniel Dyment and Daniel Boguszewski for their assistance. This project was funded by NIH grants AR46574-10 and AR56943-02.

Nomenclature

Col2/Col3 = collagen type II/collagen type III
FS = fibrous scar
H&E = hematoxylin and eosin
IVF, IVD = In vivo force, in vivo displacement
MFC/FC = mineralized fibrocartilage/fibrocartilage zones of the insertion site
NH = natural healing
NS = native strut
PT = patellar tendon
PTA = patellar tendon autograft
R = central-third repair tissue
TEC = tissue engineered construct

References

[1] Baer, G. S., and Harner C. D., 2007, "Clinical Outcomes of Allograft Versus Autograft in Anterior Cruciate Ligament Reconstruction," Clin. Sports Med., **26**(4), pp. 661–681.
[2] Galatz, L. M., Ball, C. M., Teefey, S. A., Middleton, W. D., and Yamaguchi K., 2004, "The Outcome and Repair Integrity of Completely Arthroscopically Repaired Large and Massive Rotator Cuff Tears," J. Bone Joint Surg.Series A, **86**(2), pp. 219–224.
[3] Harryman II, D. T., Mack, L. A., Wang, K. Y., Jackins, S. E., Richardson, M. L., and Matsen III, F. A., 1991, "Repairs of the Rotator Cuff: Correlation of

Functional Results With Integrity of the Cuff," J. Bone Joint Surg. Series A, **73**(7), pp. 982–989.
[4] Lafosse, L., Brozska, R., Toussaint, B., and Gobezie, R., 2007, "The Outcome and Structural Integrity of Arthroscopic Rotator Cuff Repair With Use of the Double-Row Suture Anchor Technique," J. Bone Joint Surg. Series A, **89**(7), pp. 1533–1541.
[5] Leppilahti, J., Puranen, J., and Orava S., 1996, "Incidence of Achilles Tendon Rupture," Acta. Orthop. Scand., **67**(3), pp. 277–279.
[6] Strauss, E. J., Ishak, C., Jazrawi, L., Sherman, O., and Rosen J., 2007, "Operative Treatment of Acute Achilles Tendon Ruptures: An Institutional Review of Clinical Outcomes," Injury, **38**(7), pp. 832–838.
[7] Safran, M. R., and Harner C. D., 1996, "Technical Considerations of Revision Anterior Cruciate Ligament Surgery," Clin. Orthop., **325**, pp. 50–64.
[8] Rodeo, S. A., Potter, H. G., Kawamura, S., Turner, A. S., Hyon, J. K., and Atkinson B. L., 2007, "Biologic Augmentation of Rotator Cuff Tendon-Healing With Use of a Mixture of Osteoinductive Growth Factors," J. Bone Joint Surg. Series A, **89**(11), pp. 2485–2497.
[9] Gulotta, L. V., and Rodeo S. A., 2009, "Growth Factors for Rotator Cuff Repair," Clin. Sports Med., **28**(1), pp. 13–23.
[10] Kovacevic, D., and Rodeo S. A., 2008, "Biological Augmentation of Rotator Cuff Tendon Repair," Clin. Orthop., **466**(3), pp. 622–633.
[11] Seeherman, H. J., Archambault, J. M., Rodeo, S. A., Turner, A. S., Zekas, L., D'Augusta, D., Li, X. J., Smith, E., and Wozney, J. M., 2008, "rhBMP-12 Accelerates Healing of Rotator Cuff Repairs in a Sheep Model," J. Bone Joint Surg. Series A, **90**(10), pp. 2206–2219.
[12] Rodeo, S. A., Suzuki, K., Deng, X., Wozney, J., and Warren R. F., 1999, "Use of Recombinant Human Bone Morphogenetic Protein-2 to Enhance Tendon Healing in a Bone Tunnel," Am. J. Sports Med., **27**(4), pp. 476–488.
[13] Derwin, K. A., Baker, A. R., Spragg, R. K., Leigh, D. R., and Iannotti J. P., 2006, "Commercial Extracellular Matrix Scaffolds for Rotator Cuff Tendon Repair: Biomechanical, Biochemical, and Cellular Properties," J. Bone Joint Surg. Series A, **88**(12), pp. 2665–2672.
[14] Kummer, F. J., and Iesaka K., 2005, "The Role of Graft Materials in Suture Augmentation for Tendon Repairs and Reattachment," J. Biomed. Mat. Res. Part B App. Biomat., **74**(2), pp. 789–791.
[15] Barber, F. A., Herbert, M. A., and Coons D. A., 2006, "Tendon Augmentation Grafts: Biomechanical Failure Loads and Failure Patterns," Arthroscopy: J. Relat. Surg., **22**(5), pp. 534–538.
[16] Awad, H. A., Butler, D. L., Boivin, G. P., Smith, F. N. L., Malaviya, P., Huibregtse, B., and Caplan A. I., 1999, "Autologous Mesenchymal Stem Cell-Mediated Repair of Tendon," Tiss. Eng., **5**(3), pp. 267–277.
[17] Awad, H. A., Boivin, G. P., Dressler, M. R., Smith, F. N. L., Young, R. G., and Butler, D. L., 2003, "Repair of Patellar Tendon Injuries Using a Cell-Collagen Composite," J. Orthop. Res., **21**(3), pp. 420–431.
[18] Juncosa-Melvin, N., Shearn, J. T., Boivin, G. P., Gooch, C., Galloway, M. T., West, J. R., Nirmalanandhan, V. S., Bradica, G., and Butler, D. L., 2006, "Effects of Mechanical Stimulation on the Biomechanics and Histology of Stem Cell-Collagen Sponge Constructs for Rabbit Patellar Tendon Repair," Tiss. Eng., **12**(8), pp. 2291–2300.
[19] Shearn, J. T., Juncosa-Melvin, N., Boivin, G. P., Galloway, M. T., Goodwin, W., Gooch, C., Dunn, M. G., and Butler, D. L., 2007, "Mechanical Stimulation of Tendon Tissue Engineered Constructs: Effects on Construct Stiffness, Repair Biomechanics, and Their Correlation," ASME J. Biomech. Eng., **129**(6), pp. 848–854.
[20] Juncosa-Melvin, N., Matlin, K. S., Holdcraft, R. W., Nirmalanandhan, V. S., and Butler, D. L., 2007, "Mechanical Stimulation Increases Collagen type I and Collagen type III Gene Expression of Stem Cell-Collagen Sponge Constructs for Patellar Tendon Repair," Tiss. Eng., **13**(6), pp. 1219–1226.
[21] Nirmalanandhan, V. S., Juncosa-Melvin, N., Shearn, J. T., Boivin, G. P., Galloway, M. T., Gooch, C., Bradica, G., and Butler, D. L., 2009, "Combined Effects of Scaffold Stiffening and Mechanical Preconditioning Cycles on Construct Biomechanics, Gene Expression, and Tendon Repair Biomechanics," Tiss. Eng. Part A, **15**(8), pp. 2103–2111.
[22] Juncosa-Melvin, N., Boivin, G. P., Gooch, C., Galloway, M. T., West, J. R., Dunn, M. G., and Butler, D. L., 2006, "The Effect of Autologous Mesenchymal Stem Cells on the Biomechanics and Histology of Gel-Collagen Sponge Constructs Used for Rabbit Patellar Tendon Repair," Tiss. Eng., **12**(2), pp. 369–379.
[23] Noyes, F. R., DeLucas, J. L., and Torvik P. J., 1974, "Biomechanics of Anterior Cruciate Ligament Failure: An Analysis of Strain Rate Sensitivity and Mechanisms of Failure in Primates," J. Bone Joint Surg. Series A, **56**(2), pp. 236–253.
[24] Butler, D. L., Gooch, C., Kinneberg, K. R., Boivin, G. P., Galloway, M. T., Nirmalanandhan, V. S., Shearn, J. T., Dyment, N. A., and Juncosa-Melvin N., 2010, "The Use of Mesenchymal Stem Cells in Collagen-Based Scaffolds for Tissue-Engineered Repair of Tendons," Nat. Protoc., **5**(5), pp. 849–863.
[25] Rodeo, S. A., Arnoczky, S. P., Torzilli, P. A., Hidaka, C., and Warren, R. F., 1993, "Tendon-Healing in a Bone Tunnel. A Biomechanical and Histological Study in the Dog," J. Bone Joint Surg. Series A, **75**(12), pp. 1795–1803.
[26] Wong M. W. N., 2003, "Healing of Bone-Tendon Junction in a Bone Trough," Clin. Orthop., **413**, pp. 291–302.
[27] Gelberman, R. H., Woo, S. L., and Lothringer K., 1982, "Effects of Early Intermittent Passive Mobilization on Healing Canine Flexor Tendons," J. Hand. Surg., **7**(2), pp. 170–175.
[28] Thomopoulos, S., Williams, G. R., and Soslowsky L. J., 2003, "Tendon to Bone Healing: Differences in Biomechanical, Structural, and Compositional Properties due to a Range of Activity Levels," ASME J. Biomech. Eng., **125**(1), pp. 106–113.
[29] Juncosa, N., West, J. R., Galloway, M. T., Boivin, G. P., and Butler, D. L., 2003, "In Vivo Forces Used to Develop Design Parameters for Tissue Engineered Implants for Rabbit Patellar Tendon Repair," J. Biomech., **36**(4), pp. 483–488.
[30] Malaviya, P., Butler, D. L., Korvick, D. L., and Proch, F. S., 1998, "In Vivo Tendon Forces Correlate with Activity Level and Remain Bounded: Evidence in a Rabbit Flexor Tendon Model," J. Biomech., **31**(11), pp. 1043–1049.
[31] Amiel, D., Frank, C., and Harwood F., 1984, "Tendons and Ligaments: A Morphological and Biochemical Comparison," J. Orthop. Res., **1**(3), pp. 257–265.
[32] Amiel, D., Kleiner, J. B., and Roux, R. D., 1986, "The Phenomenon of 'Ligamentization': Anterior Cruciate Ligament Reconstruction with Autogenous Patellar Tendon," J. Orthop. Res., **4**(2), pp. 162–172.
[33] Scheffler, S. U., Unterhauser, F. N., and Weiler, A., 2008, "Graft Remodeling and Ligamentization After Cruciate Ligament Reconstruction," Knee Surg. Sports Traumatol. Arthrosc., **16**(9), pp. 834–842.
[34] Yamamoto, E., Hayashi, K., and Yamamoto N., 1999, "Mechanical Properties of Collagen Fascicles from Stress-Shielded Patellar Tendons in the Rabbit," Clin. Biomech., **14**(6), pp. 418–425.
[35] Yamamoto, N., Ohno, K., Hayashi, K., Kuriyama, H., Yasuda, K., and Kaneda K., 1993, "Effects of Stress Shielding on the Mechanical Properties of Rabbit Patellar Tendon," ASME J. Biomech. Eng., **115**(1), pp. 23–28.
[36] Maeda, E., Asanuma, H., Noguchi, H., Tohyama, H., Yasuda, K., and Hayashi K., 2009, "Effects of Stress Shielding and Subsequent Restressing on Mechanical Properties of Regenerated and Residual Tissues in Rabbit Patellar Tendon After Resection of its Central One-Third," J. Biomech., **42**(11), pp. 1592–1597.
[37] Maffulli, N., King J. B., 1992, "Effects of Physical Activity on Some Components of the Skeletal System," Sports Med., **13**(6), pp. 393–407.
[38] Kannus, P., Józsa, L., Natri, A., and Järvinen M., 1997, "Effects of Training, Immobilization and Remobilization on Tendons," Scand. J. Med. Sci. Sports, **7**(2), pp. 67–71.
[39] Butler, D. L., Grood, E. S.,Noyes, F. R., Olmstead, M. L., Hohn, R. B., Arnoczky, S. P., and Siegel, M. G., 1989, "Mechanical Properties of Primate Vascularized vs. Nonvascularized Patellar Tendon Grafts; Changes Over Time," J. Orthop. Res., **7**(1), pp. 68–79.
[40] Jackson, D. W., Grood, E. S., Goldstein, J. D., Rosen, M. A., Kurzweil, P. R., Cummings, J. F., and Simon, T. M., 1993, "A Comparison of Patellar Tendon Autograft and Allograft used for Anterior Cruciate Ligament Reconstruction in the Goat Model," Am. J. Sports Med., **21**(2), pp. 176–185.
[41] Ng, G. Y. F., Oakes, B. W., Deacon, O. W., McLean, I. D., and Eyre, D. R., 1996, "Long-Term Study of the Biochemistry and Biomechanics of Anterior Cruciate Ligament-Patellar Tendon Autografts in Goats," J. Orthop. Res., **14**(6), pp. 851–856.
[42] Miyashita, H., Ochi, M., and Ikuta, Y., 1997, "Histological and Biomechanical Observations of the Rabbit Patellar Tendon After Removal of its Central One-Third," Arch. Orthop. Trauma Surg., **116**(8), pp. 454–462.